

# Faults and Fractures Detection Using a Combination of Seismic Attributes by the MLP Artificial Neural Network in an Iranian Oilfield

Reza Mohammadi<sup>1</sup> and Mohammadreza Bakhtiari<sup>2</sup>

<sup>1</sup>Amirkabir University of Technology (Tehran Polytechnic)-National Iranian Oil Company (NIOC)/National Iranian Drilling Company (NIDC)

<sup>2</sup>Amirkabir University of Technology- NIOC (EXP)

November 24, 2022

## Abstract

Faults and fractures play a significant role in drilling operations, trapping hydrocarbon, and reservoir development in oilfields; exploring faults quickly and accurately can help to reach the target more manageable. In this approach, to improve faults and fractures detection, applicable seismic attributes have been combined using a Multilayer Perceptron (MLP) neural network and applied to a 3-D seismic cube of the Changuleh oil field. First of all, high probabilistic faulted areas, as an interesting area, have been identified using a hand-picking method on a single seismic section. It is used as a pattern and one input set for the MLP neural network. Then, some single seismic attributes (e.g., Similarity, Coherency, Curvature, Instantaneous, etc.) were applied to the data. Next, the Multilayer Perceptron (MLP) neural network has been used to assess and determine the most contributed attributes. The less contributed ones are eliminated and the best seismic attributes, as another input set, combined using the MLP. Finally, the outputs of the MLP network will be two cubes named 'faulted cube' and 'non-faulted cube'. Differences between faulted zones and non-faulted zones on each cube were conspicuous, and there was no need to be interpreted manually. By comparing initial seismic sections and the MLP network's outputs, it is easy to see where the faulted and fractured zones are.

## Hosted file

essoar.10507430.1.docx available at <https://authorea.com/users/550414/articles/603976-faults-and-fractures-detection-using-a-combination-of-seismic-attributes-by-the-mlp-artificial-neural-network-in-an-iranian-oilfield>

# Faults and Fractures Detection Using a Combination of Seismic Attributes by the MLP Artificial Neural Network in an Iranian Oilfield

R. Mohammadi <sup>1,2</sup>, M. R. Bakhtiari <sup>1,3</sup>

<sup>1</sup>Amirkabir University of Technology (Tehran Polytechnic).

<sup>2</sup> National Iranian Oil Company (NIOC) (National Iranian Drilling Company (NIDC)).

<sup>3</sup> National Iranian Oil Company (NIOC) (Exploration Directorate).

Corresponding author: Reza Mohammadi (rmohammadi@aut.ac.ir)

†No. 3550, Hafez Ave, Valiasr Square, Tehran, Iran 1591634311

## Key Points

- Applying single seismic attributes on seismic section
- Combining the most applicable seismic attributes by MLP artificial neural network
- Generating interpreted *faulted cube* and *non-faulted cube* as the outputs

## Abstract

Faults and fractures play a significant role in drilling operations, trapping hydrocarbon, and reservoir development in oilfields; exploring faults quickly and accurately can help to reach the target more manageable. In this approach, to improve faults and fractures detection, applicable seismic attributes have been combined using a Multilayer Perceptron (MLP) neural network and applied to a 3-D seismic cube of the Changuleh oil field. First of all, high probabilistic faulted areas, as an interesting area, have been identified using a hand-picking method on a single seismic section. It is used as a pattern and one input set for the MLP neural network. Then, some single seismic attributes (e.g., Similarity, Coherency, Curvature, Instantaneous, etc.) were applied to the data. Next, the Multilayer Perceptron (MLP) neural network has been used to assess and determine the most contributed attributes. The less contributed ones are eliminated and the best seismic attributes, as another input set, combined using the MLP. Finally, the outputs of the MLP network will be two cubes named 'faulted cube' and 'non-faulted cube'. Differences between faulted zones and non-faulted zones on each cube were conspicuous, and there was no need to be interpreted manually. By comparing initial seismic sections and the MLP network's outputs, it is easy to see where the faulted and fractured zones are.

## Keyword

Seismic Attributes, Multilayer Perceptron (MLP) Artificial Neural Network, Coherency, Curvature, Faults, Fractures

## Plain Language Summary

Drilling toward oil and gas reservoirs at an optimum time is one of the most important parameters in operation. It is inevitable to encounter fractured areas in the drilling path. So how to find these areas before starting to drill, significantly affects the operation efficiency. Seismic attributes as indicators of these events can help to solve the issue. Using a specific type of artificial neural network to combine the seismic attributes will make outputs that indicate fractured zones.

## 1 Introduction

Oilfield development and drilling development wells are a continuous strategy in oil-bearing countries. Hence it is so important to consider to faulted zones to figure out where and in which direction wells should be drilled. Faults and fractures detection is an essential parameter in any parts of oilfields operations, including exploration, extraction, and production.

In conventional methods, interpreter has to spend too much time to detect fault and fractures visually and then should interpret them by hand-picking. If quality of the data is inadequate or the formations structure is complicated, sometimes it would be difficult or impossible for them to pick the events. For example, when faults run parallel to strike, they become more challenging to see because the fault lineaments become superimposed on bedding lineaments.

Nowadays, soft computing is used more and more to extract reservoir characterizations. Some researchers such as Taner (2001), Roberts (2001), Tingdahl et al. (2005), Aminzadeh et al. (2006), Ashraf et.al (2020) ,and Xiaoxia et.al (2020) have conducted lots of researches in these filed and their applications in different seismic objects detection.

The most general and most widely used neural network model is the Multilayer Perceptron (MLP).

Multilayer Perceptrons are the standard algorithms for any supervised learning pattern recognition process and the subject of ongoing research in computational neuroscience and parallel distributed processing. They are useful in research in terms of their ability to solve problems stochastically, which often allows one to get approximate solutions for extremely complex issues.

## 2 Study Zone

Changuleh oilfield is located in the Anaran exploration block in the south-west of Iran 'Figure.1'.

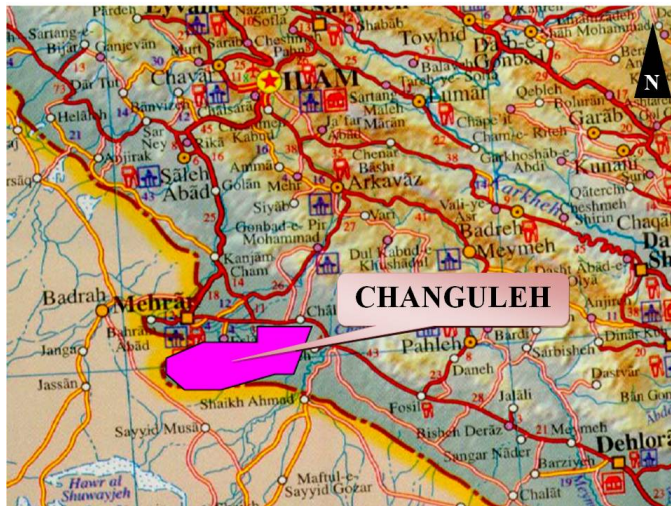


Figure 1. Location of Changuleh on the map.

The 3D seismic data used in this research belongs to this area. The Changuleh area comprises a nearly rectangular shape abutting the border with Iraq, oriented northwest-southeast with about 30 Kilometers long axis. The Area width is about 15 kilometers extending from the border up into the foothills of the Zagros Mountains. This area includes three groups of formations shown in 'Figure 2'; 1) Fars, 2) Asmari and Pabdeh, and 3) Bangestan group. Also nine horizons of these groups have been interpreted: 1) Gachsaran, 2) Asmari, 3) Kalhor, 4) Pabdeh, 5) Ilam, 6) Sarvak, 7) Lower Sarvak, 8) Kajdomi, and 9) Darian.

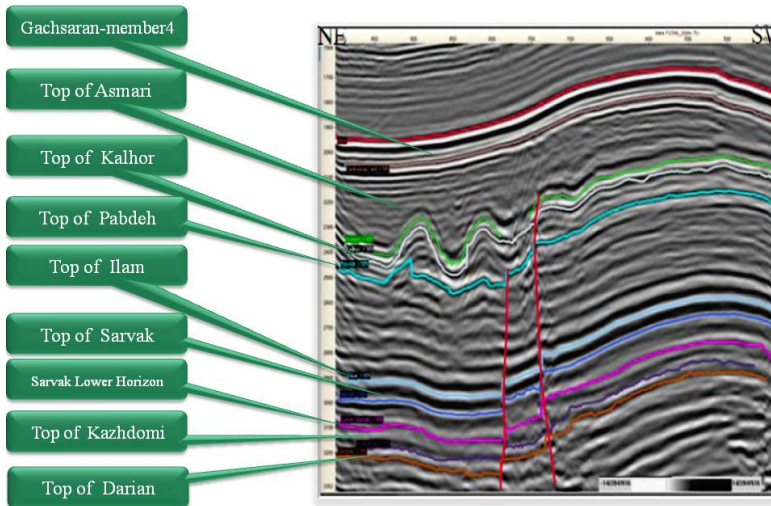


Figure 2. Three group formations of the Changuleh oilfield.

### 3 Materials and Methods

A seismic attribute is any measure of seismic data that helps us visually enhance or quantify features of interpretation interest (Marfurt & Chopra, 2007).

In the following, Single attributes (Instantaneous, Energy, Coherency, Similarity, etc.), which are used for faults and fractures detection, were described and applied to the Changuleh seismic cube.

First of all, faults were picked on a 2D seismic section, as an input pattern for neural networks, using a conventional method (hand-picking). The Changuleh seismic cube and interpreted section (In-line 122) are shown in ‘figure 3a’ and ‘figure 3b’.

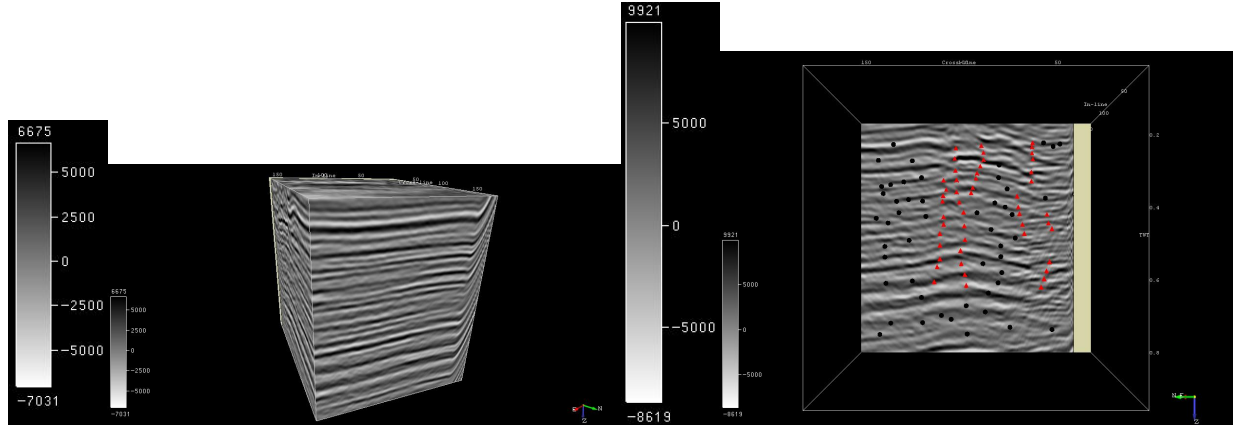


Figure 3. The Changuleh seismic cube (a) and the Interpreted seismic section (In-line 122) as a pattern for MLP (b). The red triangles and the black circles are more probabilistic zones for fault and Non-fault zones, respectively.

#### 3.1 Energy

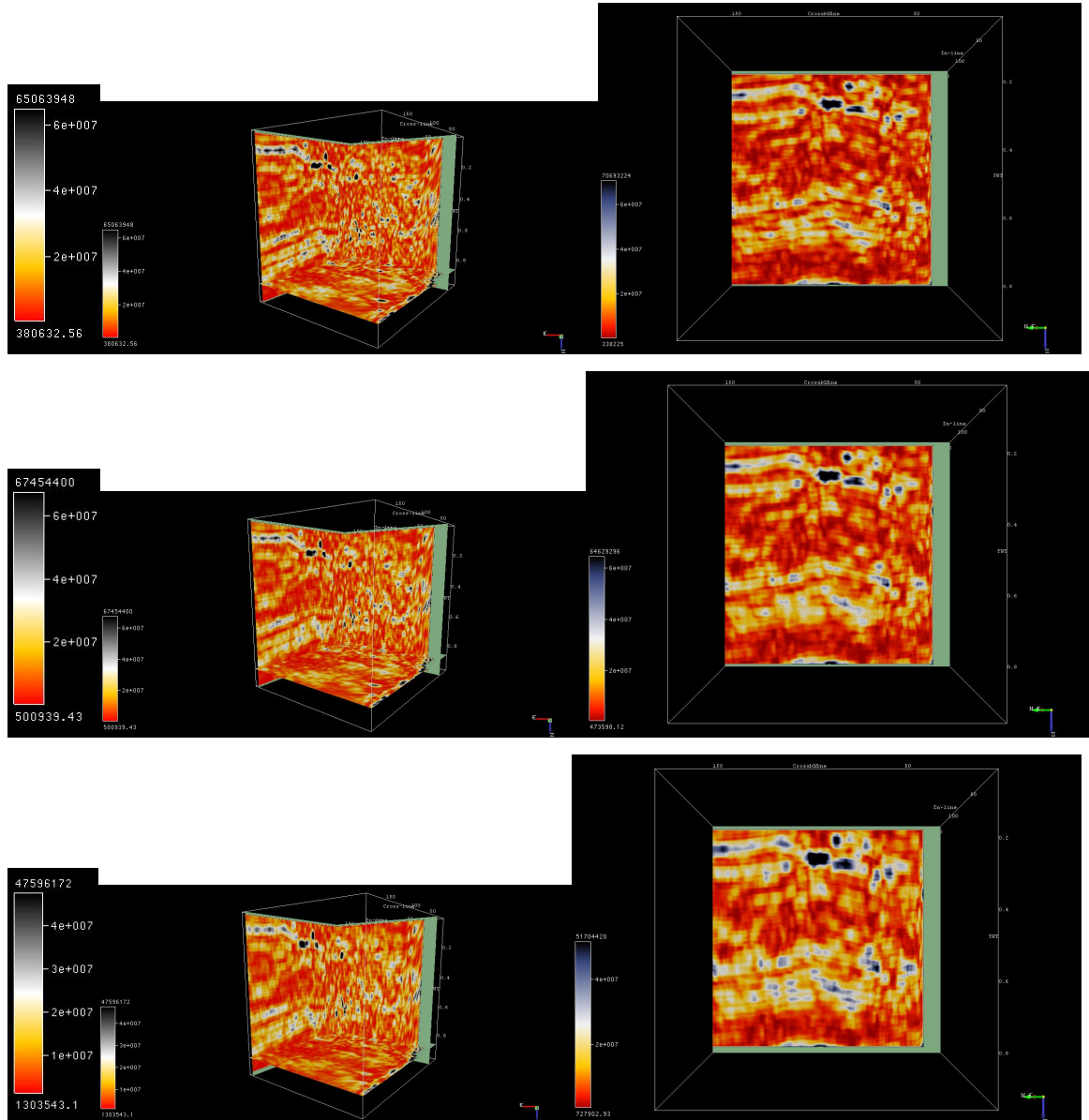
The higher the Energy, the higher the Amplitude. This attribute calculates the squared sum of the sample values in the specified time-gate divided by the number of samples in the gate. Energy is a measure of reflectivity in the specified time-gate. The Energy attribute defines as:

$$E = \frac{\sum_{i=0}^{N-1} f(t_0 + i.dt)^2}{N} \quad (1)$$

Where  $f$  is the amplitude of the trace,  $t_0$  is the upper limit of the time-gate,  $N$  is the number of samples in the gate, and  $dt$  is the sample interval (Tingdahl & de Rooij, 2005).

After evaluating the Energy attribute parameters, the best time-gates were selected. These time-gates were chosen based on their positive effect, which helps more accurate object detection in considered section (s). The results of applying

the Energy with different time-gates are shown in 'figure 4'. Areas colored in gray shows more probabilistic faulted zones because the Energy is lower than the other areas. Red regions are more probabilistic for Non-faulted zones because the Energy is higher than the other places. The Energy in faulted areas is lower than their surrounded areas, because of decrease in amplitude in these zones.



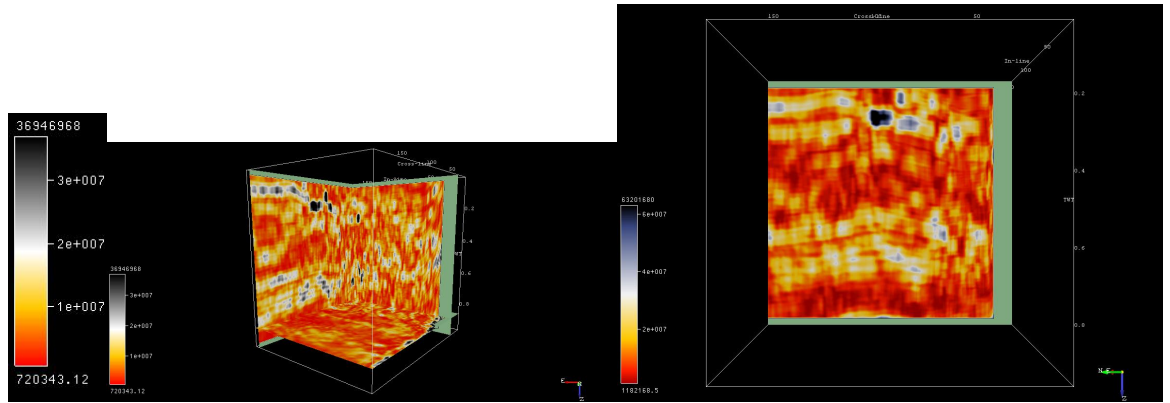


Figure 4. The Energy attribute results with four different time-gates applied to both seismic cube and the In-line 122 as an example;  $a_1$  for the seismic cube and  $a_2$  for the In-line 122 by the time gate  $[-14,+8]$  and Energy output,  $b_1$  for the seismic cube and  $b_2$  for the seismic section by the time gate  $[-14,+14]$  and Energy output,  $c_1$  for the seismic cube and  $c_2$  for the seismic section by the time gate  $[-14,+28]$  and Energy output,  $d_1$  for the seismic cube and  $d_2$  for the seismic section In-line 122 shown in figure 2 with  $[-28,+28]$  and Energy output, applied on the same In-line, cross-line and time-slice of the Changuleh seismic cube.

Input attributes with most weight and most positive effect are the most important attributes. Therefore some parameters like different time-gates and step-outs might affect desired outputs.

### 3.2 Dip Steering

Directivity is a concept in which dip and azimuth information are used to improve attribute accuracy and object detection power. Dip-steering uses the local dip and azimuth to track the event locally to the trace-segments under investigation (Tingdahl & de Rooj, 2005), so it helps us to calculate attributes with steering (e.g., coherency, similarity, curvature, etc.) more accurate. The Steering Cube contains the dip and azimuth of the seismic events in In-line and cross-line directions at every sample point. How to calculate trace dip is shown in figure (5).

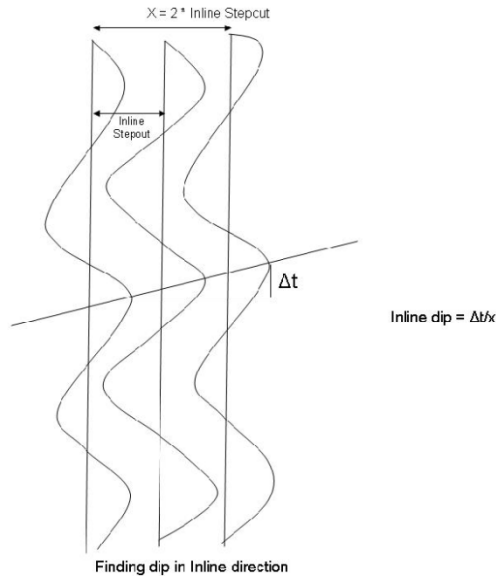


Figure 5. The algorithm looks for a maximum and minimum along the trace for calculating dip of a particular trace, alternatively. Each of these Max. or Min. events is matched with two neighboring traces, e.g., in the inline direction. The distances of the neighboring traces depend on the step-out (is the horizontal distance between two in-lines or two cross-lines). Now the difference in time values on these two neighboring traces ( $\Delta t$ ) is divided by the horizontal distance between the traces to get the inline dip ( $x$ ). The same procedure is repeated for the cross-line direction to get the cross-line dip. Then In-line dip and cross-line dip define as following:

$$\text{In-line dip} = (\Delta t)/x, \text{ cross-line dip} = (\Delta t)/y.$$

The azimuth of the dip direction is in the range of the degrees  $-180$  to  $+180$ . Positive azimuth is defined from the in-line in the trend of increasing cross-line numbers. Azimuth =  $0$  indicates that the dip is dipping in the direction of growing cross-line numbers. Azimuth =  $90$  demonstrates that the dip is dropping in the direction of increasing in-line numbers. Figure (6) shows the dip steering attribute applied to Changuleh seismic data.

Dip steering attribute is used as a prerequisite attribute for other attributes like Similarity and Coherency.

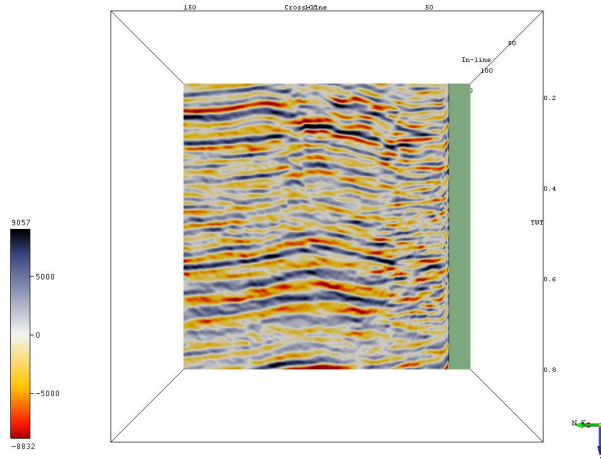
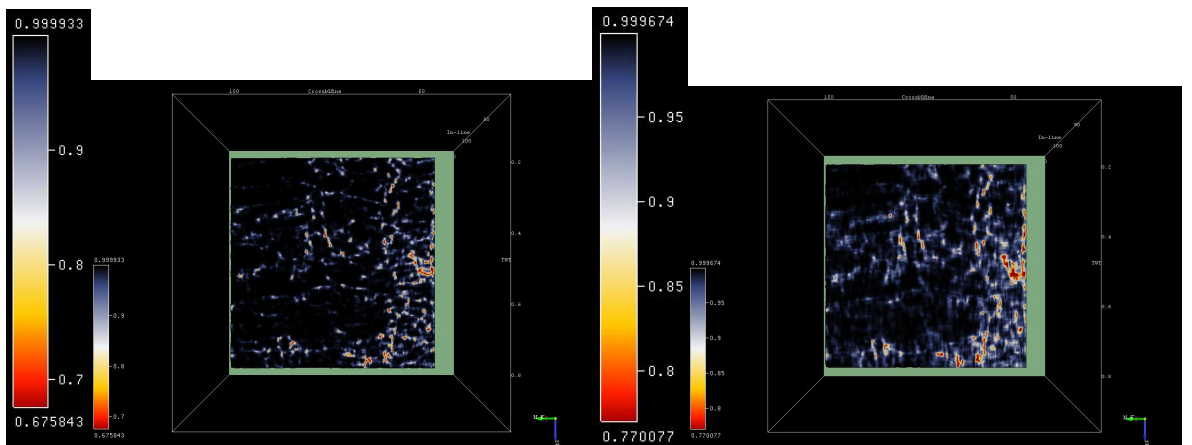


Figure 6. The dip steering attribute applied on the in-line 122.

### 3.3 Coherency

Coherence or Coherency is a term used for a set of algorithms ascertaining how much adjoining traces are alike. Chopra et al. (2000) found that faults and fractures can be detected by taking advantage of azimuthal fluctuation of coherence. Here cross-correlation Coherency is used to find more discontinuities. This type shifts one of the traces up and down to see the maximum cross-correlation (usually three traces for this type). This attribute thus enhances variations in seismic data related to changes in continuity among neighboring traces. The mathematics of the Coherency attribute is mentioned in appendix A.

Figure 7 shows the results of the Coherency for different time-gates and the Coherency cube. Probabilistic faulted areas are shown in red and yellow with less coherency.



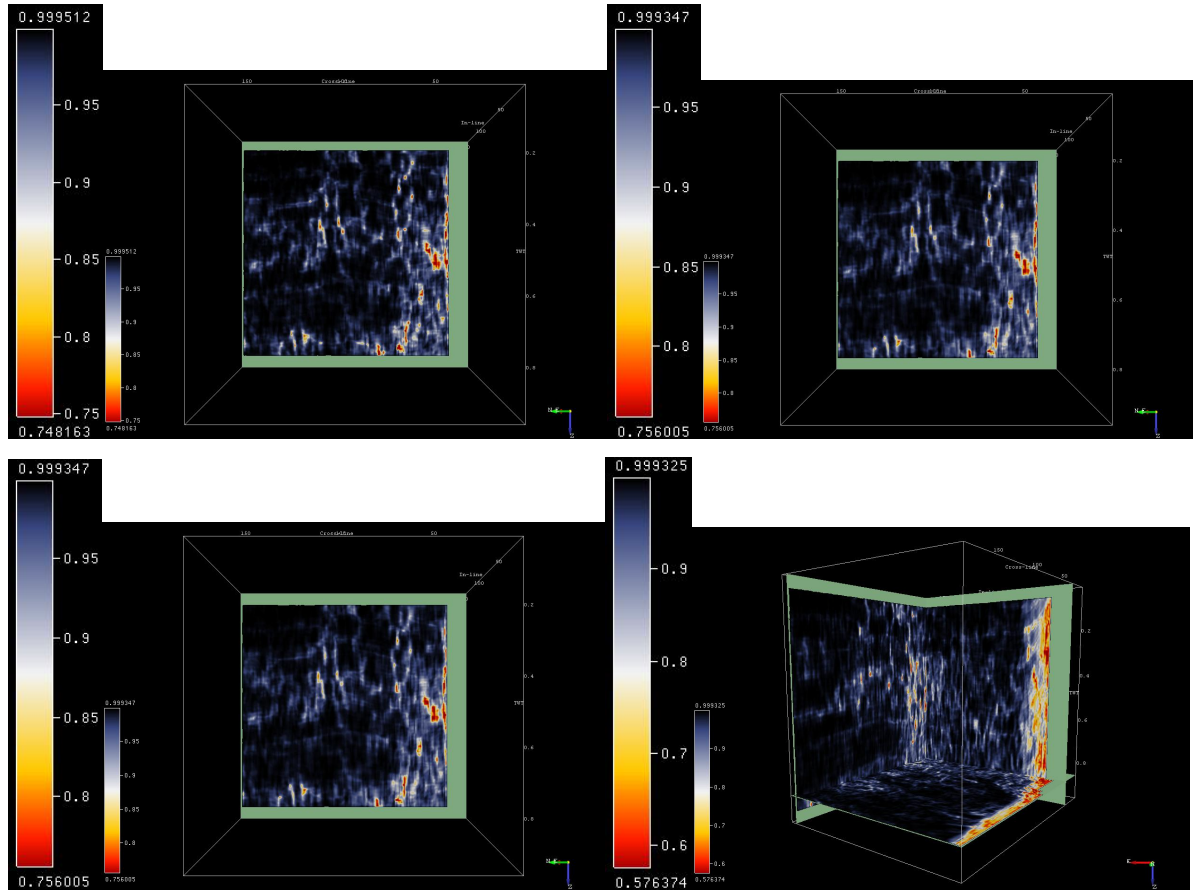


Figure 7. The Coherency attribute results with different time-gates for In-line 122 (a with time-gate [-8,+8], b with time-gate [-14,+14], c with time-gate [-14,+28] , d with time-gate [-28,+14] and e with time-gate [-28,+28]) and the Coherency cube (f) with time-gate [-28,+28]. The maximum dips that were selected for all of them are 250 (us/m).

### 3.4 Similarity

Similarity is a form of "coherency" that expresses how much two or more trace segments look alike. The Similarity of 1 means the trace segments are entirely identical in waveform and amplitude, while the Similarity of 0 means they are completely dissimilar. Compared with the traditional coherence (Bahorich & Farmer, 1995), similarity also takes into account the amplitude differences between the two trace-segments. Faults are discontinuities in the data that give a low response to the similarity. This attribute is defined as (Tingdahl & de Rooj, 2005):

$$S = 1 - \frac{|v-u|}{|v|+|u|} \quad (2)$$

Where

$$\begin{array}{c}
 f(t_1, x_v, y_v) \\
 f(t_1 + dt, x_v, y_v) \\
 \vdots \\
 \\
 f(t_2, x_v, y_v) \\
 \\
 \\
 f(t_1, x_u, y_u) \\
 f(t_1 + dt, x_u, y_u) \\
 \vdots \\
 \\
 f(t_2 - dt, x_u, y_u) \\
 f(t_2, x_u, y_u)
 \end{array}$$

$t$  is the time-depth of investigation,  $dt$  is the sampling interval, and  $t_1$  and  $t_2$  are the limits of the time gate.  $(x_v, y_v)$  and  $(x_u, y_u)$  are the two trace positions that are to be compared, and  $f(t, x, y)$  is the amplitude value in the cube, and  $V$  and  $U$  are vectors, which are functions of amplitude. It means Similarity is defined as one minus the Euclidean distance between the vectors, normalized over the vector lengths.

A computing of the Similarity attribute for a reference trace (0, 0) is shown in ‘Figure 8’ schematically; it shows each trace has a local position and depends on a reference trace. Some attributes need dip steering as a prerequisite attribute; these attributes like Similarity can use an extension mode called a full block, which can be applied to data in a cube. Therefore using the full block as an extension makes all possible trace pairs (in the in-line and cross-line directions and the two diagonals) in the rectangle to be computed. Hence after applying the Similarity to the seismic cube and computing it in full steering and full block mode and investigating whole data cube, the result can be processed as Similarity cube.

The Similarity attributes in different time-gates and the Similarity cube properties are shown in ‘Table 3’. ‘Figure 9’ shows the results of Similarity and Similarity cube.

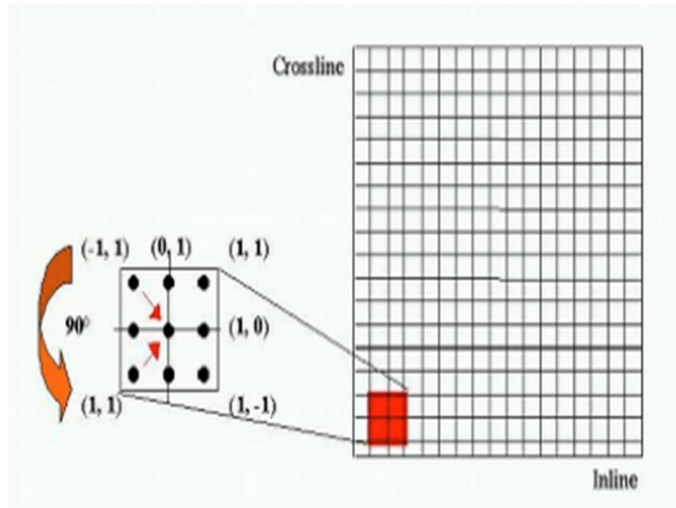
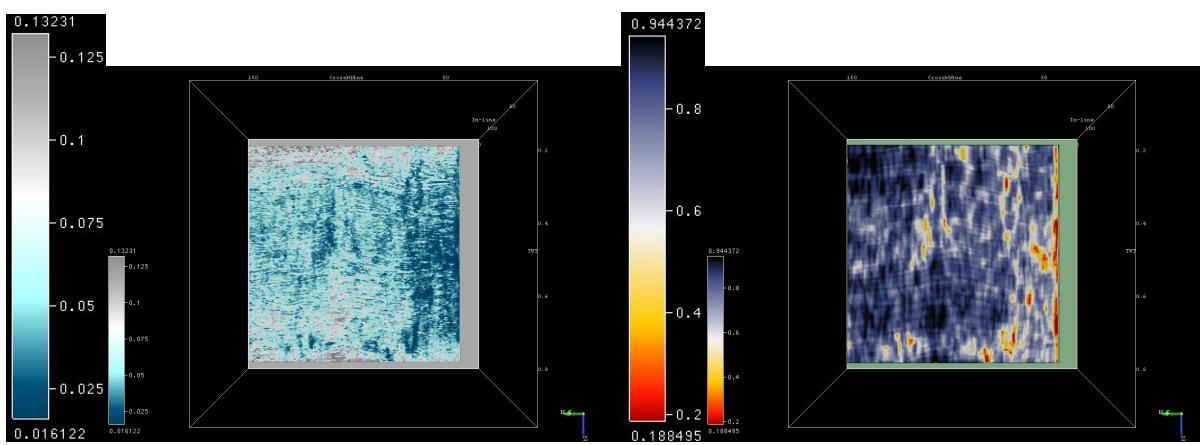
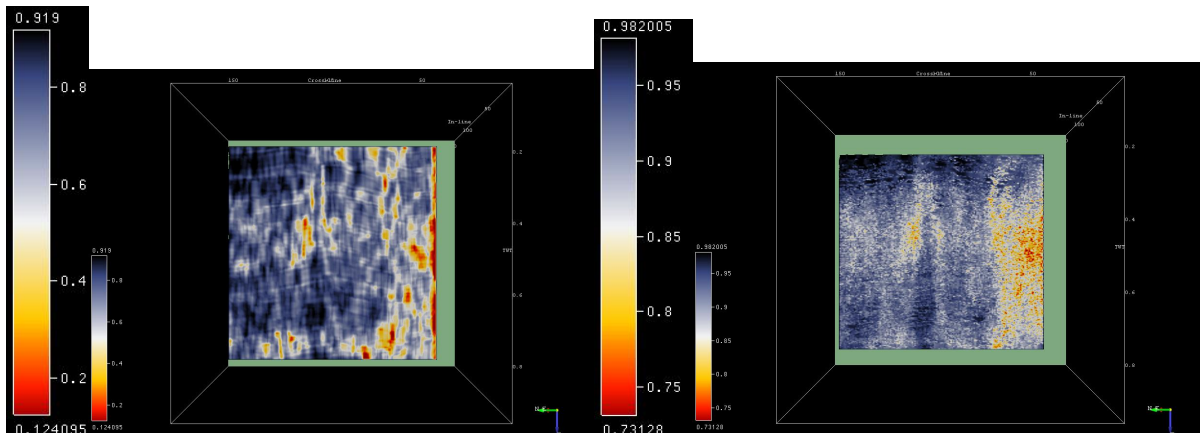
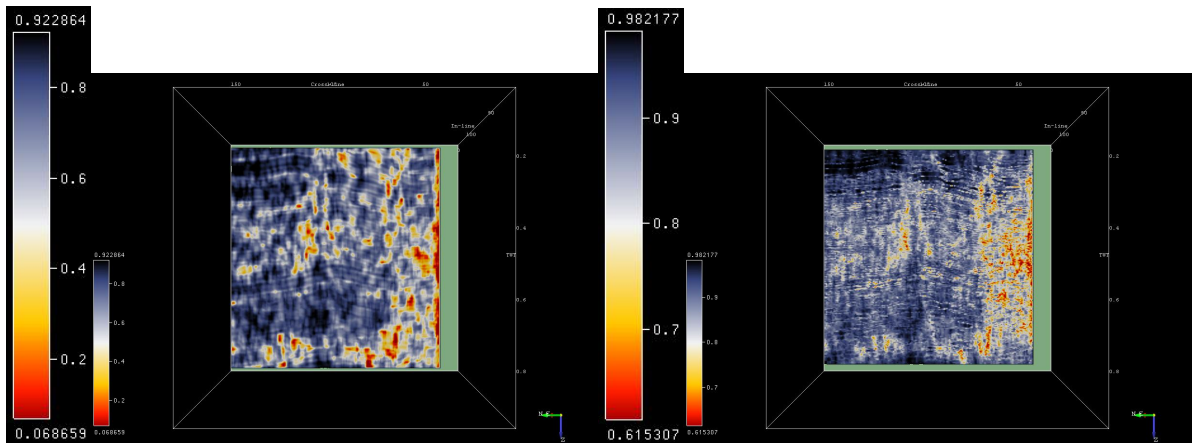


Figure 8. Definition of trace position related to the reference trace (0, 0).

Table 3. The Similarity attributes with different time-gates and the Similarity cube properties. The “Step-out” is equal to the trace position; the first number refers to in-line, and the second one refers to the cross-line number. “None steering” means that local dip and azimuth have not been computed. “Full steering” means that local dip and azimuth have been computed for all traces in the seismic cube. “Output” for ‘6e’ is a statistic variance of Similarities for all traces in the cube.

Figure	Attribute	Lateral Position	Other Settings
6a	[-14,+14]	Step-out (1,1)	Full block and None Steering
6b	[-24,+32]	Step-out (1,1)	Full block and Full Steering
6c	[-28,+32]	Step-out (1,1)	Full block and None Steering
6d	[-32,+14]	Step-out (1,4)	Full block and Full Steering
6e	[-32,+32]	Step-out (1,1)	Full Steering, Output=Variance
6f	[-28,+28]	Mirror 90 degree (0,1)(0,-1)	None Steering
6g	[-56,+38]	Step-out (2,5)	Full block and Full Steering
6h	Similarity Cube[-14,+14]	Step-out (1,1)	Full block and Full Steering



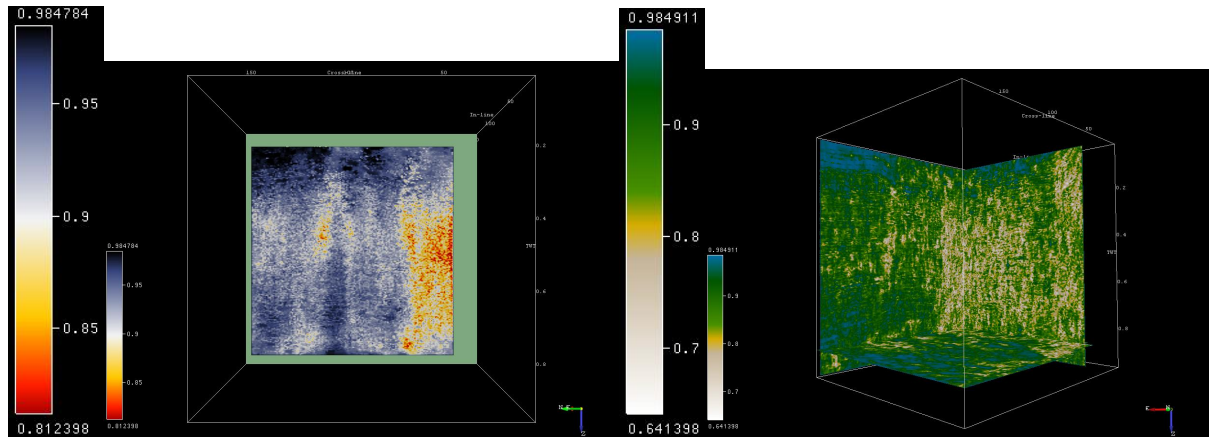


Figure 9. The Similarity attribute results for different time-gates applied to In-line 122 of the Changuleh seismic cube. The lowest values in every color bar show the probability of the fault zone. Different colors in the Similarity attribute with variance output (e) and the Similarity cube (h) used to prove fault zones more transparent.

### 3.5 Curvature

Curvature is a measure of how curved a surface is at a particular point and highly relevant to the second derivation of the surface. The more bent a surface is, the larger its curvature (Chopra & Marfurt, 2007). Curvature is a family of attributes that characterizes the local shape of a horizon. Robert (2001) describes that the curvature attribute is tremendously impact on extracting geometrical characteristics such as fault and fractures. The curvature is an adequate attribute to identify small scale faults and fractures with few movements that would impossible to be detected with the other fracture attributes like similarity or coherency. The most sufficient faults and fracture detection attributes are most positive and most negative carvatures. Here most positive, most negative, maximum, and minimum curvature are used as single attributes. The definition of 2D Curvature is shown in 'Figure 10'.

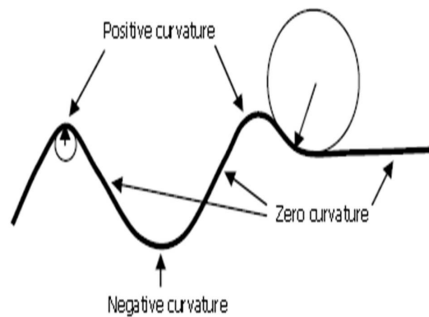


Figure 10. An illustrated definition of 2D curvature. Anticlinal features have

positive curvature, synclinal features have negative curvature, and planar features (horizontal or dipping) have zero curvature (Chopra & Marfurt, 2007).

The most negative curvature returns to the infinite number of normal curvatures that exist. This attribute is shown in 'figure 11'.

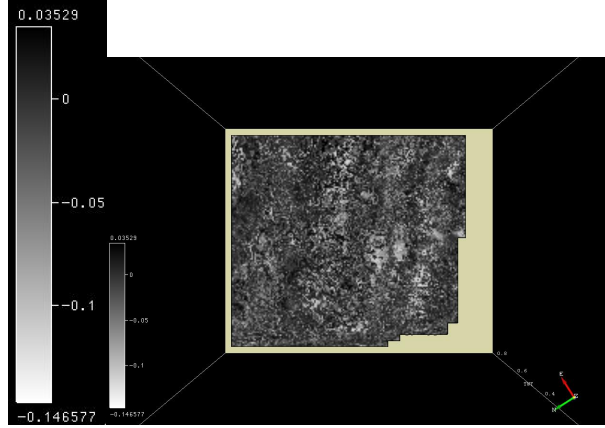


Figure 11. The most negative curvature applied to time-slice 844.

### 3.6 Instantaneous Attributes

Every signal in the time domain is a combination of a series of frequencies in the furrier domain that has a real part and imaginary part. This signal is:

(4)

Where  $f(t)$  is real,  $f^*(t)$  is an imaginary part, and  $A(t)$  is instantaneous Amplitude.

The real seismic trace  $f(t)$  can be expressed in terms of a time-dependent amplitude  $A(t)$  and a time-dependent phase  $(t)$  as (Taner et al., 1979):

$$f(t) = A(t) \cos(t) \quad (5)$$

$$f^*(t) = A(t) \sin(t) \quad (6)$$

Where  $A(t)$  and  $(t)$  are define as:

$$A(t) = [f^2(t) + f^{*2}(t)]^{1/2} = F(t) \quad (7)$$

$$(t) = \tan^{-1}[f^*(t)/f(t)]$$

And  $t$  is the instantaneous phase. Cosine of the instantaneous phase is:

$$\text{Cosine of phase} = \cos((t)) \quad (8)$$

Derivation of instantaneous phase depends on time is equal to instantaneous frequency:

$$w(t) = d(t)/dt \quad (9)$$

### 3.6.1 Instantaneous Phase

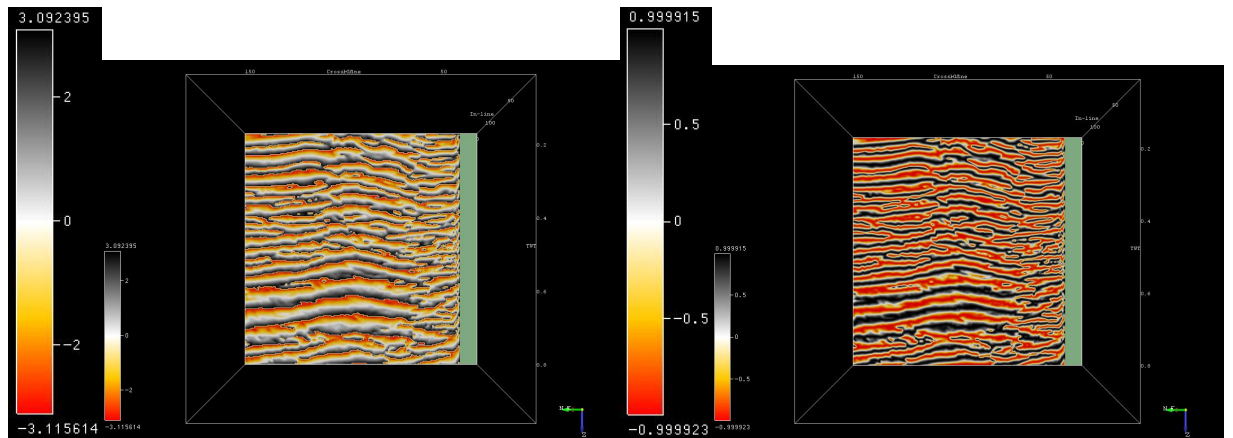
This attribute calculates the instantaneous phase at the sample location; it emphasizes spatial continuity/discontinuity of reflections by providing a way for weak and strong events to appear with equal strength. This attribute is of central importance since it describes the location of events in the seismic trace and leads to the computation of other instantaneous quantities. The instantaneous phase makes events clearer. It is effective for highlighting the discontinuities of reflectors, faults, pinch-outs, angularities, and bed interfaces. 'Figure 12a' shows the result of applying this attribute on In-line 122. Discontinuities are indicated clearly, on the right-hand side of the section.

### 3.6.2 Cosine of Instantaneous Phase

Cosine of the instantaneous phase has the same uses as the instantaneous phase with one additional benefit: It is continually smooth. The conclusion of this attribute for In-line 122 is shown in 'Figure 12b'. As 'figure 12a', discontinuities are shown on the right and middle of the section.

### 3.6.3 Instantaneous Frequency

The instantaneous frequency attribute responds to both wave propagation effects and depositional characteristics. Hence it is a physical attribute and can be used as a useful discriminator. It can be used as Fracture zone indicator, since fractures may appear as lower frequency zones. This attribute is applied to In-line 122; 'figure 12c' shows the result. As mentioned, lower frequency zones shown in red have more probability of being faulted zone.



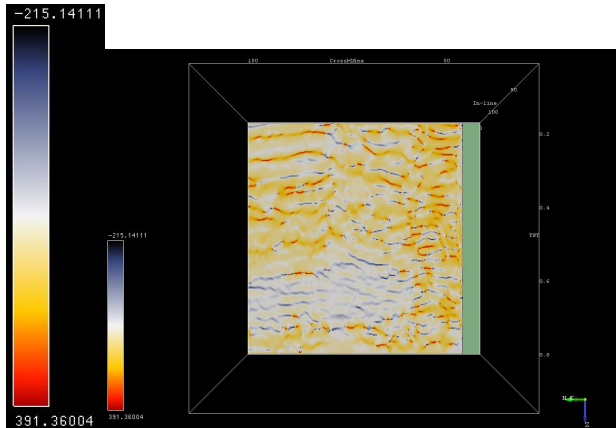


Figure 12. Instantaneous Phase (a), Cosine of Instantaneous Phase (b), and Instantaneous Frequency (c).

Selecting different individual attributes with unique abilities in faults and fractures detection and then applying them to the data will help to define the best set of attributes to be integrated using an MLP neural network.

### 3.7 Neural Network

In a Multilayer Perceptron (MLP), the perceptrons are organized in layers. In its simplest form, there are three layers since Hornik et al. (1988) proved that a three-layer network could model any arbitrary continuous function. The “back-propagation”, learning algorithm that is widely used to train this type of networks, attempts to minimize the error between the predicted network result and the known output by adjusting the weight of the connections (Aminzade & deGroot, 2006).

MLPs have two properties of interest: abstraction and generalization. Abstraction is the ability to extract the relevant features from the input pattern and discard the irrelevant ones. Generalization allows the network, once trained, to recognize input patterns that were not part of the training test.

This type of neural network is in a supervised class and fully connected network. A fully connected MLP network is shown in ‘figure 13’.

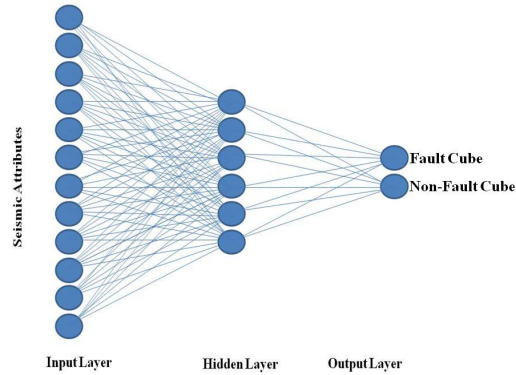


Figure 13. Schematic representation of the MLP neural network.

The MLP was designed with one input layer involves 12 input variables, six nodes in the hidden layer, and two outputs. All the selected attributes at all picked points should be computed by the neural network to be able to create a training set. Also, 30% of all data are used for “test set” creation. Neural network training was stopped when the misclassification didn’t change; after the training, the network gives weight to every single attribute. Total misclassification was 39.49%. The Less contributed seismic attributes have been eliminated, and the most contributed are selected as the input variables for Artificial Neural Network (MLP).

Table 4 shows the seismic attributes that have been applied to the data and used as the input variables of the artificial neural network, based on their weights, respectively.

Table 4. The seismic attributes were used as MLP inputs, based on their weight, respectively.

Seismic attribute	Time-gate (ms)	Lateral Position	Other Settings
Energy	[-14,+28]	-	-
Similarity Cube	[-14,+14]	Full Block	Output= max, Full Steering
Frequency	[-14,+14]	-	Output= dominant Freq.
Instantaneous	-	-	Output= Amplitude
Curvature	-	Step-out 3	Min. Curvature, Full Steering
Energy	[-28,+28]	-	-
Coherency	[-28,+28]	-	Max Dip= 250 (us/m)
Position	[-12,+12]	(0,0)	Full Steering, Output= Energy
Curvature	-	Step-out 3	Max. Curvature, Full Steering
Curvature	-	Step-out 3	Mean. Curvature, Full Steering
Dip Steering	-	-	Output= Cross-line Dip
Dip Steering	-	-	Output= In-line Dip

Then, the single attributes were integrated using a neural network, produce two outputs called *faulted cube* and *non-faulted cube*, ‘figure 14’.

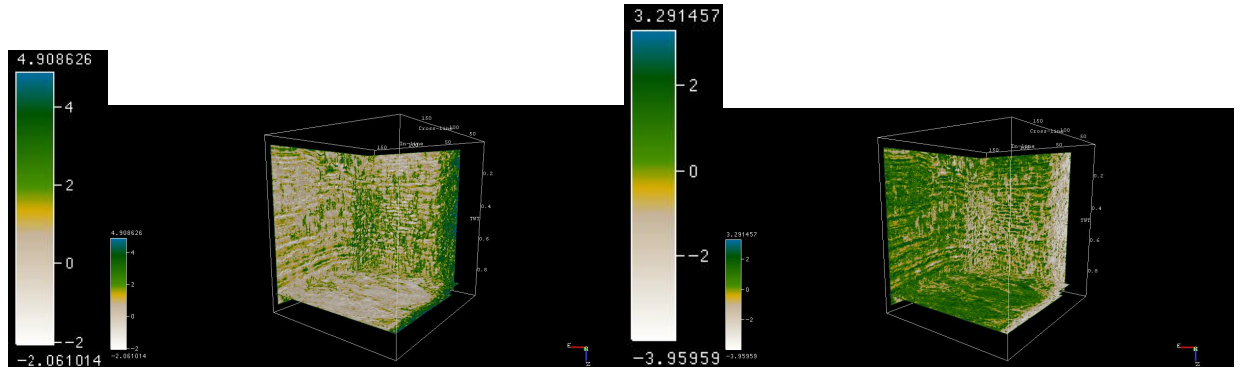
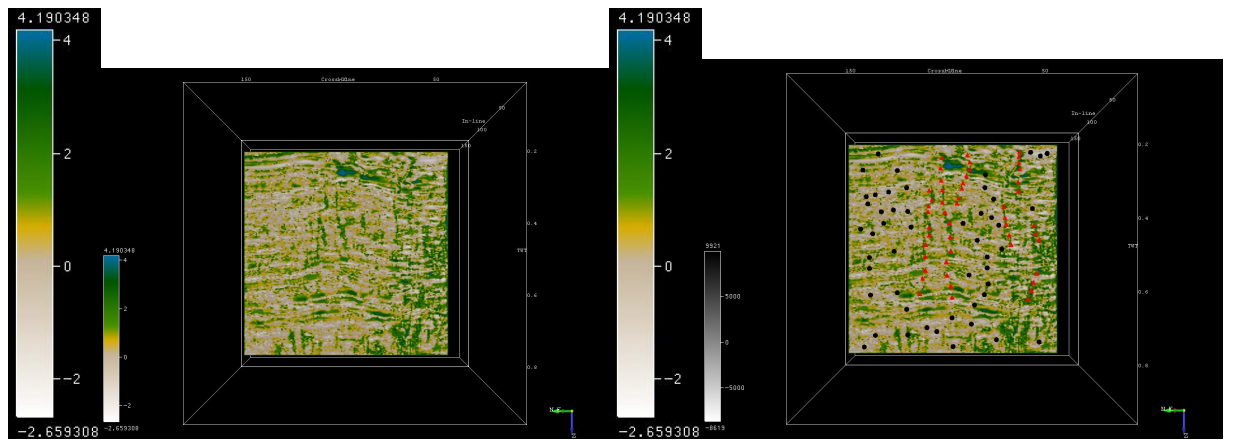


Figure 14. The MLP Neural Network Outputs. In the *faulted cube*, the green-colored areas is the most probabilistic faulted zone (a), and in the *non-faulted cube*, the green-colored areas is the most probabilistic Non-faulted zone (b).

By comparing the interpreted section, shown in ‘figure 3a’, and the MLP outputs for In-line122, demonstrated in ‘figure 15a’, it will be easy to find faulted and non-faulted areas more precisely. Also, it would be the same for a comparison of these two outputs by the results of the other single attributes.

‘Figure 16’ shows the procedures that applied to the Changuleh seismic cube to achieve the results.



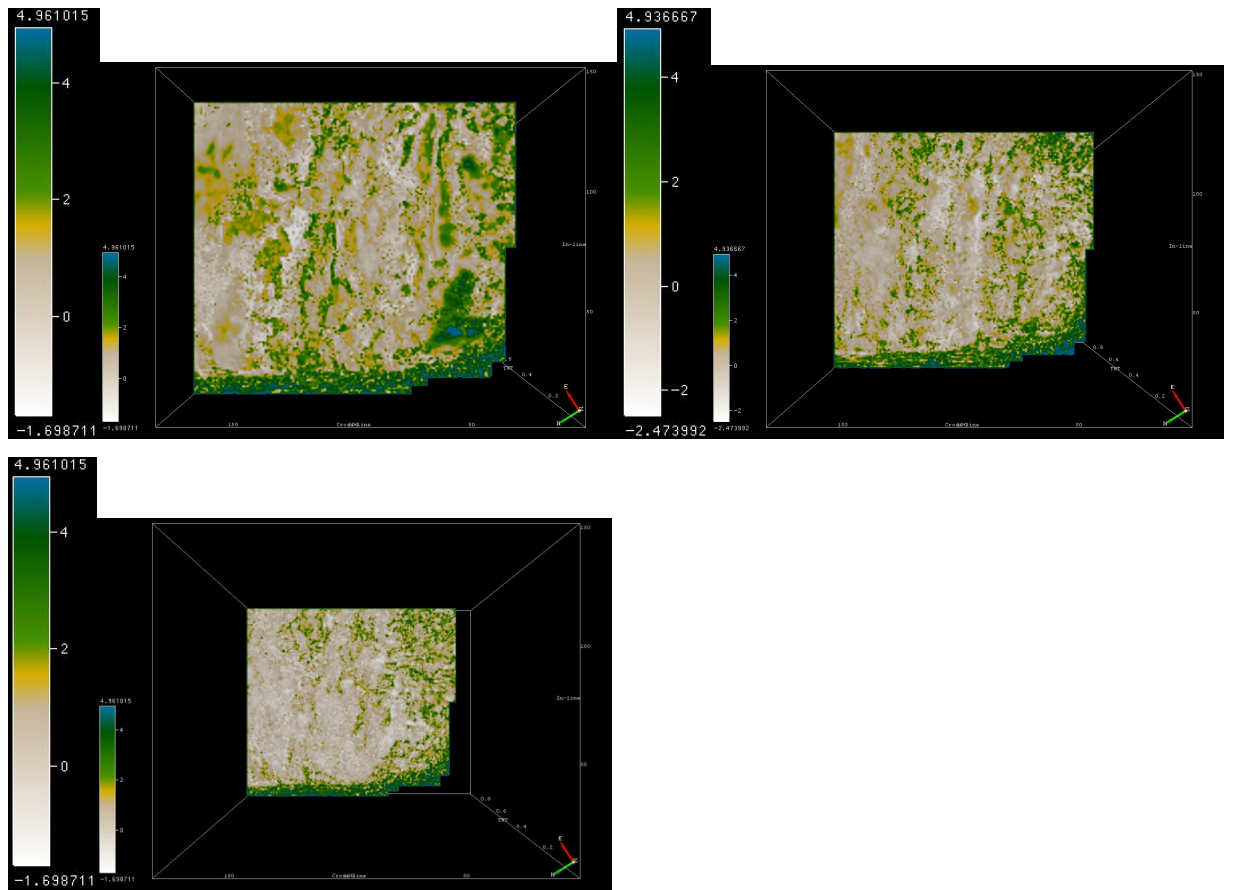


Figure 15. The faulted cube applied to In-line 122 without the interpretation pick-sets (a) on In-line 122, with interpretation pick-sets (b), and on the time slices number 200 (c), 476 (d), and 844 (e).

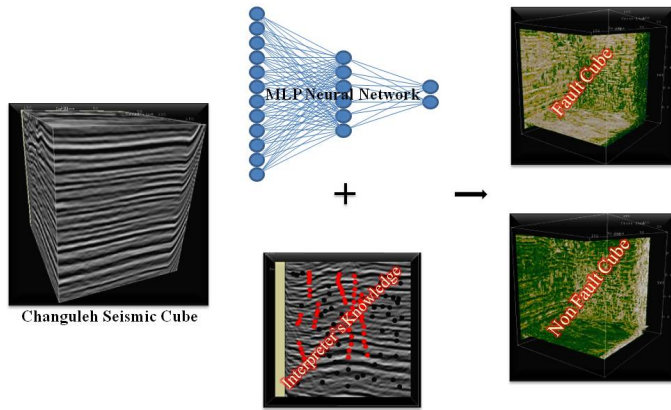


Figure 16. Schematic representation of the procedures that applied to the Changuleh seismic cube.

#### 4. Conclusion

Detecting faults in this way is more precise and less time consuming than the other fault detection methods (e.g., single attributes, Coherency, Similarity, Energy, etc.).

The neural network spent more time to understand the relations between the attributes. However, in theory, all the attributes could be used as the inputs of the neural network. Still, the problem is that increasing seismic attribute numbers causes swelling of the training time without improving the network efficiency. Hence, optimizing the number of seismic attributes would help the network to be more concentrated on the critical relations and increases efficiency.

This method can be used to detect more other seismic objects such as sequence stratigraphy to find out stratigraphic traps and gas chimney, etc.

Comparing this type of neural network with other Networks (e.g., Radial Basis Function (RBF), and Unsupervised Vector Quantizer (UVQ), etc.) could cause to find out the performance of MLP in seismic object detection.

#### 5. Acknowledge

This project is supported by the Petroleum Engineering and Development Company (PEDEC), so the authors thank Dr. H.Noruzi, head of the R&D department, Mr. S.Noruzi, and Mr. Mardi. Also, we would like to thank Professor de Groot from dGB earth science for preparing the academic license of OpendTect software.

#### 6. Appendix

Some additional about the Coherency attributes write by following:

There are three conventional methods for calculating the Coherency: Cross-correlation, Semblance, Eigenstructure. The cross-correlation that mentioned above is explained here.

If the target trace slide by an amount  $\tau_x$  and define a vertical analysis window to range between  $\pm K$  samples above and below the analysis point at time  $t$ , the normalized cross-correlation coefficient  $\rho_x(t, \tau_x)$  would be:

$$\rho_x(t, \tau_x) = \frac{\sum_{k=-k}^{+k} [u_1(t+k, t-\tau_x) - \mu_1(t-\tau_x)] \{ [u_0(t+k, t) - \mu_0(t)] \}}{\sqrt{\left\{ \sum_{k=-k}^{+k} [u_0(t+k, t) - \mu_0(t)]^2 \right\} \left\{ \sum_{k=-k}^{+k} [u_1(t+k, t-\tau_x) - \mu_1(t-\tau_x)]^2 \right\}}} \quad (\text{A.1})$$

Where

$$\langle u_n \rangle(t) = \frac{1}{2k+1} \sum_{k=-k}^{+k} u_n(t+k, t) \quad (\text{A.2})$$

denotes the running-window mean of the  $n$ th trace. Because it is known that the true mean of properly processed seismic data is 0, to make the computational simplification assume  $\langle u \rangle(t) = 0$ . That is a reasonable approximation if the analysis window is greater than a seismic wavelet ‘figure A1’ and ‘figure A2’. The  $\rho_y(t, \tau_y)$  in cross-line direction calculates in the same way.

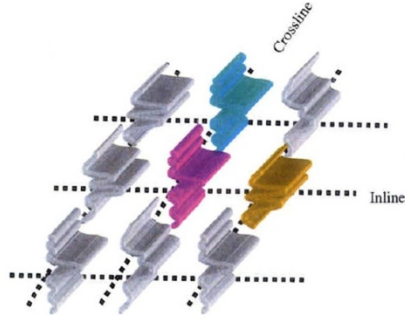


Figure A1. Spatial (multi-trace) analysis windows commonly used in coherency calculation for the cross-correlation algorithm (Marfurt & Chopra, 2007).

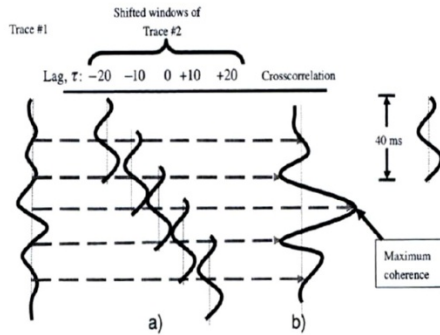


Figure A2. schematic diagram showing the cross-correlation between two traces. a) Trace number 1 is held fixed while a window of trace number 2 (here, 40ms) is slid along at a suite of time lags and is cross-correlated. The delay having the maximum signed cross-correlation is a crude measure of in-line (or cross-line) dip. b) The cross-correlation value that corresponds to this peak is then used in equation (A.3) to generate 3D estimate coherence (Marfurt & Chopra, 2007).

In the cross-correlation algorithm, the target trace (in magenta) first cross-correlated with the in-line trace (in orange) over a suite of temporal lags. Then the same process repeats between the target trace and the cross-line trace (in cyan). The coherence estimation obtains using equation (A.3):

$$C_{xc} \equiv \sqrt{[\max \rho_x(t, \tau_x, x_i, y_i)][\max \rho_y(t, \tau_y, x_i, y_i)]} \quad (\text{A.3})$$

## 7. References

- Aminzadeh, F. & Connolly, D. (2003) Seismic Meta-Attributes as a Practical Exploration Tool: Gas Chimney and Fault Volumes, Search and Discovery Article, No. 40101.
- Anderson, D. and McNeill, G. (1992) Artificial Neural Networks Technology, 1-71.
- Ashraf, U.; Zhang, H.; Anees, A.; Nasir Mangi, H.; Ali, M.; Ullah, Z.; Zhang, X. (2020) Application of Unconventional Seismic Attributes and Unsupervised Machine Learning for the Identification of Fault and Fracture Network, Applied Science, , 10, 3864.
- Bakhtiari, M. R. and Riahi, M. A. (2009) Gas Chimney Identification using the Integration of Seismic Attributes, Journal of Seismic Exploration, **18**, 43-56.
- Bahorich, M. and Farmer, S. (1995) The Coherence Cube. The Leading Edge 14, 1053-1058.
- Chopra, S. & Marfurt, K. (2007) Seismic Curvature Attributes for Mapping Faults/Fractures, and other Stratigraphic Features, CSEG Recorder. 37- 41.
- Chopra, S. (2002). Coherence Cube and beyond. First Break, 20.1, January, 27-33.
- Chopra, S., Sudhakar, V., Larsen, G., & Leong, H. (2000). Azimuth-based Coherence for detecting faults and fractures. Journal of World Oil, September, 57-62.
- dGB Beheer B.V. (2009) OpendTect dGB Plugins User Documentation (version 4.0), dGB Earth Sciences.
- Fang, J., Zhou, F., Tang, Z. (2017) Discrete Fracture Network Modelling in a Naturally Fractured Carbonate Reservoir in the Jingbei Oilfield, Energies , 10, 183.
- Helbig, K. and Tretel, S. (2001) Computational Neural Network for Geophysical Data Processing, edited by Poulton, 3- 24.

Hornik, K., Stinchcombe, M., & White, H. (1988). Multilayer Feedforward Networks are Universal Approximators (Discussion Paper 88-45). San Diego, CA: Department of Economics, University of California, San Diego.

LPEB International Iran Kish, Crew 2257. (2007) Final Seismic Data Acquisition Report In Changuleh Area, Iran For NIOC-EXP, Contract No. 84148 1 part1 3 11 64 73 74 part2 98.

Marfurt, K. and Chopra, S. (2007) Seismic Attributes for Prospect Identification and Reservoir Characterization, *Stephen j*, 1 2 48-51 55 56 59 209 - 211 264 - 278 362.

Roberts, A. (2001) Curvature Attributes and Their Application to 3D Interpreted Horizons, *First Break*, 19(2), February, 85-100.

Taner, M. T., Koehler, F. and Sheriff, R. E. (1979) Complex Seismic Trace Analysis, *Geophysics*, **44**, No. 6, 1041-1063.

Tingdahl, K. and de Rooj, M. (2005) Semi-automatic Detection of Fault in 3-D Seismic Data, *Geophysical Prospecting*, **53**, 533-542.

Zhang, X., Yu, J., Li, N., and Wang, C. (2020) Multi-scale Fracture Prediction and Characterization Method of a Fractured Carbonate Reservoir, *Journal of Petroleum Exploration and Production*, 11, November.